Integration of electrostatic and fluid dynamics within a dust devil

W. M. Farrell,[1] N. Renno,[2] G. T. Delory,[3] S. A. Cummer,[4] and J. R. Marshall[5]

Received 7 July 2005; revised 9 September 2005; accepted 5 October 2005; published 28 January 2006.

[1] In this study we derive an analytical expression to describe the electrostatic field in a dust cloud with grain trajectories defined by fluid dynamics and grain charging via contact electrification. In order to solve for the electric field, we merge the fluid dynamic–driven grain motion directly into the basic electrostatic formalism to end up with an electric field dependent on meteorological variables within the dust cloud. We find that the *E* field is driven by two processes: the currents associated with the charging grains and the increasing velocity difference of varying-sized grains at early times. The resulting processes give rise to an exponentially growing electric field, which for Mars applications, quickly approaches breakdown values. Variations in the growth of the electric field are found with varying grains sizes and varying ambient atmospheric conductivity.

Citation: Farrell, W. M., N. O. Renno, G. Delory, S. Cummer, and J. R. Marshall (2006), Integration of electrostatic and fluid dynamics within a dust devil, *J. Geophys. Res.*, *111*, E01006, doi:10.1029/2005JE002527.

1. Introduction

[2] The atmospheric dynamics of both Earth and Mars are such that small dust grains can get lifted into the atmosphere and become part of larger convective vortex structures called dust devils. Dust devil grains of various compositions and sizes in contact with each other will generate and exchange charge via a process called ''triboelelectic charging'' [*Eden and Vonnegut*, 1973]. It was recently demonstrated that electric fields near and within dust storms are coherent and large, but with fluid dynamics still the dominant force determining grain trajectories [*Farrell et al.*, 2004]. In this paper, we will integrate fluid dynamics into electrostatic models to allow a quantification of dust devil electric fields solely on the basis of meteorological parameters.

[3] The surface-atmosphere interface of both the terrestrial deserts and Mars contain small loose grains that can be lifted into saltation and suspension by both horizontal [*Greeley et al.*, 1981, 1992] and vertical [*Renno et al.*, 1998] winds. On Earth, horizontal shear stresses from wind gusts are a well-known particle lifting mechanism [*Schmidt et al.*, 1998]. However, dramatic grain lifting occurs in small-scale atmospheric convection features called dust devils, which produce a negative vertical pressure gradient at the surface-atmosphere interface and hence vertical winds capable of lifting smaller grains directly from the surface [*Greeley et al.*, 2003].

[4] On Earth, dust devils tend to have heights of a few hundred meters and widths on the order of tens of meters [*Renno et al.*, 1998]. These ''minitornados'' consist of cyclostrophic winds (where centripetal forces balance pressure gradient) on the order of $10-30\ \mathrm{m\ s^{-1}}$, have warm cores with center temperature increases as high as 4°C relative to ambient temperature, and central pressure decreases on the order of a few millibars below ambient pressure [*Renno et al.*, 1998; *Farrell et al.*, 2004]. The vertical winds created by the upward directed hot fluid elements in the central region tend to lift particle grains of various sizes. These winds also act as a mass stratification mechanism, with smaller, lighter grains tending to be lofted higher than the larger, heavier grains.

[5] The formation of dust devils is associated with an intrinsic atmospheric instability. Specifically, under intense direct sunlight, the fluid near the ground heats up because of diffusive heat transfer and absorption of thermal radiation emitted by the ground. This temperature stratification with cooler, denser gas overtop the warmer, less dense gas is naturally unstable. The instability manifests itself as convective plumes and vortices (when a source of vorticity is present). The dust devil is a visible manifestation of a vortex that has lifted dust and sand directly off of the surface. In these vortices, warmer air from the ground travels upward in the central region, and cooler air is pulled downward both within the core and in regions surrounding the vortex. Dust entrained in the upward moving fluid elements gives rise to the opaque central region. *Renno et al.* [1998] has suggested that, in a Lagrangian sense, the downdrafted cool air in the outer regions gets ground heated as these fluid elements are drawn inward to the dust devil center, to then propagate upward again in the central region, thus forming a heat engine with the ground as the primary energy source. This mechanism has also been proposed to explain waterspouts [*Renno and Bluestein*, 2001].

[6] Much like in terrestrial deserts, the arid Martian lower atmosphere and surface heating can result in a temperature

[1]NASA Goddard Space Flight Center, Greenbelt, Maryland, USA.
[2]Atmospheric, Oceanic and Space Sciences, University of Michigan, Ann Arbor, Michigan, USA.
[3]Space Sciences Laboratory, University of California, Berkeley, California, USA.
[4]Department of Electrical and Computer Engineering, Duke University, Durham, North Carolina, USA.
[5]SETI Institute, Mountain View, California, USA.

0148-0227/06/2005JE002527

inversion [*Zurek et al.*, 1992], and this along with loose surface sediments can lead to dust devil formation. Observations from both orbit [*Thomas and Geirasch*, 1985; *Edgett and Malin*, 2000; *Cantor*, 2003] and landers [*Ryan and Lucich*, 1983; *Murphy and Nelli*, 2002] indicate the presence of dust devils, structurally similar to those of Earth, but of vastly greater scale with heights nearing 10 km and widths upward of a few kilometers. These large vortices are more similar to terrestrial thunderstorms in their volumetric extent. *Cantor et al.* [2003] studied the size distribution of dust storms and found that a small percentage can exceed 10^6 km^2 in areal size, being more regional in nature.

[7] On Mars, dust devils and dust storms play a significant role in Martian meteorology and geology, increasing global atmospheric temperatures during dust storm season and transporting significant amounts of material about the planet [*Greeley et al.*, 1992]. Even in nonstorm season, dust devils are now considered the primary mechanism for atmospheric dust loading when global/regional storms are not present [*Smith and Lemmon*, 1999].

[8] While fluid forces dominate dust dynamics, grains colliding with each other will exchange charge via contact electrification or triboelectricty. Laboratory studies [*Eden and Vonnegut*, 1973; *Ette*, 1971; *Mills*, 1977; *Sickafoose et al.*, 2001] indicate that electrical effects can be quite substantial and under low Martian-like pressures can result in glow and filamentary optical discharges (creation of a collisional plasma). Dust charging experiments on the space shuttle [*Marshall*, 1994] indicate that electric forces dominate in a microgravity environment, with the grains coalescing into long filaments due to grain dipole effects.

[9] The grain-grain electrical interaction is complicated [*Desch and Cuzzi*, 2000], with charge being exchanged on the basis of both composition and size. For grain compositions involving material with vastly different work functions, such as metals and insulators, the contact electrification process is particularly active with negative charge tending to accumulate with the metal (and corresponding positive charge on the insulator) in a grain-grain interaction. However, if grain compositions are comparable, the grain size determines charge polarity with smaller grains tending to become negatively charges (and heavier grains positive charged) in grain-grain collision [*Ette*, 1971]. Because of grain tribocharging, any aeolian feature including wind blown fronts [*Schmidt et al.*, 1998], dust devils [*Delory et al.*, 2002], and dust storms, will be electrical in nature: mixing dust and electricity are systemic processes.

[10] Because of the vertical velocity inside dust devils, smaller grains of negative charge tend to get lofted relative to the heavier, positive grains. Consequently, aeolian features that have a mass stratification process (upward winds, downward gravity) will develop well-separated charging centers in the dust storm, giving rise to an overall storm dipole electric field. The process is similar to the situation in thunderstorms where light ice of positive charge is blown upward relative to heavier, negatively charged ice and rain [*Mathpal et al.*, 1980; *Volland*, 1984].

[11] The observation of a dipole electric field structure around dust devils was first reported by *Freier* [1960] and *Crozier* [1964] with electric field variations on the order of 10–500 V m^{-1} found externally (many tens of meters) from the features. In the summer of 2000–2003, the Mars Atmosphere and Dust in the Optical and Radio (MATADOR) campaign undertook a systematic study of the electrical and meteorological features in convective dust storms [*Houser et al.*, 2003; *Farrell et al.*, 2003; *Renno et al.*, 2004; *Farrell et al.*, 2004]. Along with the classic meteorological features of a dust devil, including cyclostrophic winds, warm cores, and central pressure decreases, substantial electrostatic voltage changes were observed on the order of 2000 V in a few meters. Dust devils also passed directly over DC electric field meters with observation in excess 4 kV m^{-1} and as large as 20 kV m^{-1} in the interior region [*Delory et al.*, 2002; *Farrell et al.*, 2004].

[12] Fluid wind and gravity forces drive grain dynamics inside dust devils. Electricity is generated as a consequence of this fluid force but not at strengths to alter grain trajectory [*Farrell et al.*, 2004]. To date there has not been a complete analytical theory that combines the fluid properties of the dust devils with the subsequent generation of electric fields, creating an expression E(P, V, T), with P, V and T being atmospheric pressure, temperature and wind velocity, respectively. *Melnik and Parrot* [1998] presented a simulation of the process, using fluid forces to move grains, then calculating associated electrostatic fields in the simulation box. *Farrell et al.* [2003] modeled the electrostatic field development on the basis of the relative movement between small, negative grains and large, positive grains, E (v_{small}, v_{large}). However, that analysis did not include the fundamental fluid forces creating small/large-grain movement. In this work, we will complete the association of fluid and electrical forces, deriving the development of the dust devil electric field as a function of more basic meteorological variables.

2. Electrostatic Model

[13] In order to couple electrical and fluid models, we start with the electrostatic formalism that leaves a dependency of electric field on differential grain velocity. This grain velocity is then solved via fluid formalism to derive E as a function of the driving vertical winds.

[14] The electric field will be derived on the basis of the flow of vertical currents [*Farrell et al.*, 2003], with the upward flow of negative smaller grains representing one current source and the flow of positive larger grains representing another current source. The concept is parallel to the development of electrostatic fields in thunderstorms based on one-dimensional (vertical) current flow from upward positive light ice and downward negative graupel and raindrops [*Mathpal et al.*, 1980; *Kuettner et al.*, 1981; *Volland*, 1984]. For this work, the derivation will initially parallel that of *Farrell et al.* [2003], but will deviate when considering the relative velocity of the grains. The development of the dust devil electric field, E, can be obtained from the continuity equation as

$$dE/dt = -J/\varepsilon_o, \tag{1}$$

where the current density is

$$J = n_L Q_L v_L + n_S Q_S v_S + \sigma E, \tag{2}$$

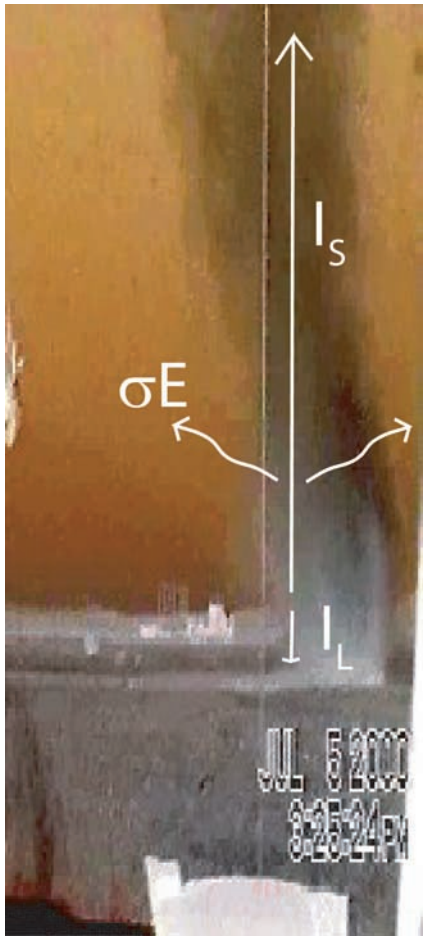

Figure 1. False color picture of a dust devil in Nevada, with small-grain, large-grain, and atmospheric dissipation currents superposed.

with $n_{L,S}$ are the number density of the large and small particles, respectively, $Q_{L,S}$ are the charge on the large and small particles, respectively, $v_{L,S}$ are the vertical velocities of the large and small particles, respectively, σ is the local atmospheric conductivity and ε_o is the free space permittivity. The σE term represents the current dissipation into the atmosphere. An illustration of these currents is shown in Figure 1. While we anticipate the development of charge centers within the devil, we also expect that the overall charge in the devil to have a net value of zero, making $n_L Q_L = -n_S Q_S$ and

$$J = n_L Q_L \Delta v + \sigma E, \tag{3}$$

where $\Delta v = v_L - v_S < 0$ is the differential velocity between large and small grains. A similar assumption is applied in thunderstorm charging [*Mathpal et al.*, 1980]. While charge neutrality is applied and the system is treated as closed, in reality some charge may escape, and a discussion of the relaxing of charge neutrality is presented in the conclusions. Equations (1)–(3) are identical to *Farrell et al.* [2003]. We now place equation (3) back into equation (1) and time differentiate, now assuming $\Delta v = \Delta v(t)$, and not uniform in time as was performed previously [*Farrell et al.*, 2003]. The differential equation governing the temporal evolution of the electric field is then

$$E^{//} + \sigma E^{/}/\varepsilon_o = -n_L\left(Q_L^{/}\Delta v + Q_L \Delta v^{/}\right)/\varepsilon_o, \tag{4}$$

where the "/" indicates the time differentiation operation, d/dt. The time rate of change of charge on the large grain is $Q_L^{/} = \nu \Delta q$ where ν is the grain-grain collision frequency and Δq is the charge exchange in each collision. The collision frequency between large and small grains is $\nu = \pi r_L^2\, \Delta v\, n_S$ and Δq have been estimated for grains of similar composition [*Melnik and Parrot*, 1998] and varying composition [*Desch and Cuzzi*, 2000], and a contrast of the two models has been presented by *Farrell et al.* [2003]. We shall assume that charge exchange is for large and small grains of differing compositions [*Desch and Cuzzi*, 2000], making

$$\Delta q \sim 2668(\Delta\Phi/2V)(r_f/0.5\mu m)e, \tag{5}$$

where r_f is the reduced radius, $r_f = (r_L^{-1} + r_S^{-1})^{-1} \sim r_S$. In the calculations, we assume that the triboelectric potential between larger grains and smaller grains is $\Delta\Phi \sim 2V$ (i.e., large grains are insulators, while small grains are metallic, making small grains charge negative on collisions [*Desch and Cuzzi*, 2000]).

[15] The differential equation (4) has two driving terms associated with the development of two different currents: The first current, $Q_L^{/}\Delta v$, is associated with changing grain charge moving at constant differential velocities, and the second current $Q_L \Delta v^{/}$ is associated with charged grains undergoing differential acceleration. *Farrell et al.* [2003] assumed that the differential velocities were constant at all times, and hence only included the first term in their model. However, we now relax the constant differential velocity assumption, and find that the second current term appears in the derivation for $\Delta v = \Delta v(t)$. This $Q_L \Delta v^{/}$ term is important in the early part of dust devil formation. As we demonstrate in the next section, Δv varies with time in a complicated way during the early period of dust lifting and this second current term now couples this acceleration into the electric field formalism.

[16] In the most general sense, the importance of the Δv cannot be understated: This differential particle velocity is dependent upon the lifting process associated with the fluid, and via equation (4) links the electrostatic formalism to the fluid properties of the medium, particularly wind speed, V. We now directly connect E to wind speed V.

3. Fluid Model

[17] In order to derive a differential velocity dependent on vertical wind speed, $\Delta v = \Delta v(V)$, we need to solve for the motion of the large and small grains under the influence of lift from a vertical wind and downward directed gravitational acceleration. We assume a priori that the wind speeds are large such that the drag coefficient on the grain is near unity and that the particle sizes are dust-like (<20 μm) rather than sand-like. This second assumption implies that shear stress forces will not be as strong as the vertical wind force on a grain. *Greeley et al.* [2003]

reported on a laboratory vortex chamber study that found that grains larger than 60 μm appear to be lifted predominately by horizontal shear stresses while smaller grains appear lifted from forces from the vortex pressure gradient. We only include forces from vertical winds resulting from a vortex vertical negative pressure gradient. The force of winds on the grain is expressed as [*Anderson*, 1987; *Melnik and Parrot*, 1998]

$$F_W = \pi r^2 \rho_a (V - v)^2, \tag{6}$$

where r is the grain radius, ρ_a is the atmospheric density, V is the wind speed, and v is the grain speed. As described in equation (6), the force is greatest when the particle is stationary, and progressively decreases as the grain becomes increasingly entrained in the winds (i.e., becoming zero when the grain is moving with the fluid).

[18] Assuming a population of large grains near one size and mass, and a second population of small grains of vastly differing size and mass, one can write the equation of motion for the two populations as

$$dv_S/dt = -g + \pi r_S^2 \rho_a (V - v_S)^2 / m_S \tag{7}$$

and

$$dv_L/dt = -g + \pi r_L^2 \rho_a (V - v_L)^2 / m_L, \tag{8}$$

where m is the grain mass. For the sake of simplicity, we ignore cohesion effects on a surface that can be considered an additional term of negative force. We assume the dust is easily lifted from the surface in the negative pressure gradiant/vertical winds of the dust devil. The first-order differential equations, equations (7) and (8), can be solved by reformatting the equations into the form

$$dv_S/\left(c_S v_S^2 + b_S v_S + a_S\right) = dt \tag{9}$$

and

$$dv_L/\left(c_L v_L^2 + b_L v_L + a_L\right) = dt, \tag{10}$$

which is a standard integral solved with the initial condition that $v_S = 0$ and $v_L = 0$ at $t = 0$. The constant terms are $a_{L,S} = -g + c_{L,S}V^2$, $b_{L,S} = -2Vc_{L,S}$, and $c_{L,S} = \pi r_{L,S}^2 \rho_a / m_{L,S}$, respectively.

[19] The solution of equations (7) and (8) has the form

$$v_S = -P_S(1 - \exp(W_S t))/2c_S(1 - R_S \exp(W_S t)) \tag{11}$$

and

$$v_L = -P_L(1 - \exp(W_L t))/2c_L(1 - R_L \exp(W_L t)), \tag{12}$$

where

$$P_{S,L} = -2V\, c_{S,L} + W_{S,L} \tag{13}$$

$$M_{S,L} = -2\, V\, c_{S,L} - W_{S,L} \tag{14}$$

$$R_{S,L} = P_{S,L}/M_{S,L} \tag{15}$$

and

$$W_{S,L} = \left(4g c_{S,L}\right)^{1/2}. \tag{16}$$

We now have the movement of the large and small grains based exclusively on the vertical winds and intrinsic grain properties.

[20] The factor W in the exponent of equations (11) and (12) represents a reaction inverse time of a grain to become entrained with the wind. Initially, the particle speed increases linearly, but after approximately 1/W, the particle moves at a nearly constant velocity (always below the driving wind speed, V). Figure 2 shows the movement of large (20 μm) and small (1 μm) grains in a 7 m s^{-1} vertical wind in a Martian-like surface atmosphere (ρ_a = 1.6 × 10^{-2} kg m^{-3}, and g = 3.7m s^{-2}). Note that the reaction time of the smaller grains, that time to reach constant velocity, is shorter than that of the larger grains. The differential velocity between small and large grains ($-\Delta v$) shows an exponential rise to a peak near 0.75 s, a decrease over the next 2 s, and a constant value thereafter. At large times, the grain velocity for both large and small components becomes quasi-constant defined by

$$v_{L,S} = V - W_{L,S}/\left(2c_{L,S}\right) = V - g^{1/2}/c_{L,S}^{1/2}. \tag{17}$$

Note that small, lighter grains obtain final velocities closer to the actual wind speed than their more massive counterparts. At large times, the differential velocity is constant being $\Delta v = g^{-1/2}\,(c_L^{-1/2} - c_S^{-1/2})$.

[21] The movement of the particles is now defined by the planet (gravitational acceleration, surface atmospheric density), particle (size and density) and finally local vertical wind speed, V. The vertical wind speed in a convective dust devil or storm has been theoretically derived by *Renno and Ingersoll* [1996] and *Renno et al.* [2000] applying a heat engine model to naturally convective processes. *Renno and Ingersoll* [1996] assumed that work done by buoyancy forces around a convective circulation is equal to the work available from the convective heat engine. *Renno et al.* [2000] used this idea to calculate the maximum temperature fluctuation associated with convective plumes. In steady state, the work done by buoyancy forces balances that due to friction forces and the vertical velocity is given by

$$V = \kappa^{-1}(g\ H\ \Delta T/T)^{1/2}, \tag{18}$$

where κ is an eddy viscosity parameter, g is the gravity acceleration, T is the absolute temperature, ΔT is the temperature perturbation is the dust devil, and H is the boundary layer depth. Thus the vertical velocity is functionally related to the temperature difference between the dust devil core and the background atmosphere and the depth of the convective layer (or the heat input and the heat engine efficiency) and inversely related to the coefficient of turbulent dissipation of mechanical energy [see *Renno and Ingersoll*, 1996; *Renno et al.*, 2000]. Thus the vertical wind speed inside the dust devil is a function of the driving energy processes and their efficient conversion to fluid kinetic energy, and these most basic

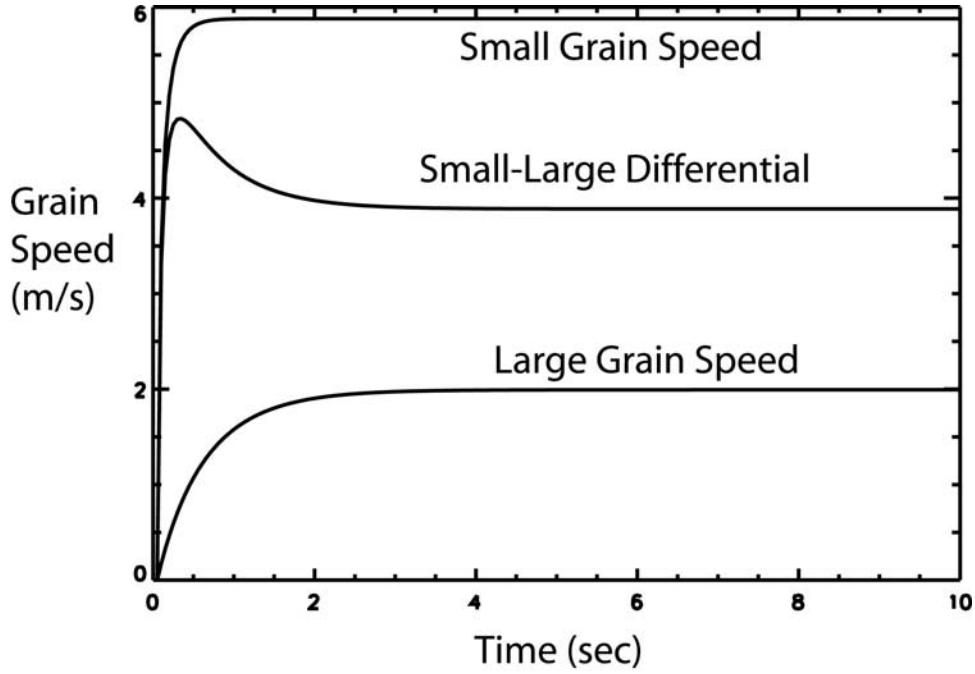

Figure 2. Vertical speed of small and large grains and their differential speed in a 7 m s^{-1} vertical wind. The small grains have a 1 μm radius, and large grains have a 20 μm radius. The case is run for a Martian-like atmosphere, with atmospheric density of 1.6×10^{-2} kg m^{-3}.

parameters can be used to derive the expected electric field via equations (11)–(16).

[22] Given equations (11)–(16), there is now enough information to derive $\Delta v = v_L - v_S$ on the basis of grain properties and wind velocity. As mentioned, past calculations [*Farrell et al.*, 2003] assumed Δv was constant for all times. However, as shown in Figure 2, this assumption is not accurate during dust devil formation. With the new formalism herein, we now have the ability to more accurately derive electric field values in the early formation of a dust devil or convective dust storm, where the differential speed of the large and small grains is varying in a complicated way.

4. Integration of Electrostatics and Dynamics

[23] Equations (4) and equations (11)–(16) were combined and solved using the Runge-Kutta method. Figure 3 illustrate the evolution of dust devil electrostatic field in a Martian-like atmosphere for wind speeds of 7 m s^{-1}. The small grains were assumed to have a 1 μm radius and the large grains to have 20 μm radius. The grain density was assumed to be 50 cm^{-3} for small grains and 1 cm^{-3} for large grains. The atmospheric conductivity for Mars is assumed to be 2.5×10^{-12} S/m, about 80 times larger than that of Earth surface atmospheric conductivity [*Cummer and Farrell*, 1999]. The small and large grains were modeled having differing compositions such that their triboelectric potential difference, $\Delta\Phi$, was 2V. A comparison of electrostatic field versus assumed triboelectric potential, $\Delta\Phi$, was presented previously by *Farrell et al.* [2003]. The $\Delta\Phi = 2V$ value gives rise to substantial charge exchange (~5000e) upon each grain-grain collision, and is a value that gives congruent electrostatic behavior between both the *Melnik and Parrot* [1998] and the *Desch and Cuzzi* [2000] triboelectric formalism.

[24] Note that the electric fields become large in a fairly short period of time, with breakdown fields of 25 kV/m obtained in about 15 s after initiation of the vertical winds. While effects of breakdown are difficult to predict, we anticipate that breakdown will initiate strong atmospheric electric currents (greatly exceeding the modeled σE values) that act to neutralized the excessive buildup of separating grain charge. Because an added current term(s) is required in equation (2) to incorporate breakdown, the model presented herein does not accurately model fields in Mars applications above ~25 kV m^{-1} (the atmospheric breakdown field for Mars).

[25] As discussed above, there are two driving terms that give rise to the electric field, the first from a grain charging current, $n_L Q_L' \Delta v$, and the second from a grain acceleration current, $n_L Q_L \Delta v'$. Figure 4 shows the effect of the two terms on the solution. Specifically, both terms $Q_L' \Delta v + Q_L \Delta v'$ are modeled in top curve A while only the $Q_L' \Delta v$ term is modeled in the bottom curve B. Note that the acceleration-related electric current generates an electric field that rises more quickly in the early stages of dust lifting, giving rise to *E* fields as much as 10 times larger than those produced with $Q_L' \Delta v$ alone after 10 s. The two cases begin to approach each other at longer times, when the system is driven primarily by $Q_L' \Delta v$.

[26] While not modeled here, the exponential-like growth of the electric field will not carry on forever, and some mechanism will feedback into the process to ultimately limit electric field growth (i.e., a saturation mechanism). One mechanism for field limitation is corona. Atmospheric currents will greatly increase (greatly exceed σE) in association with *E* fields near breakdown levels. These electric

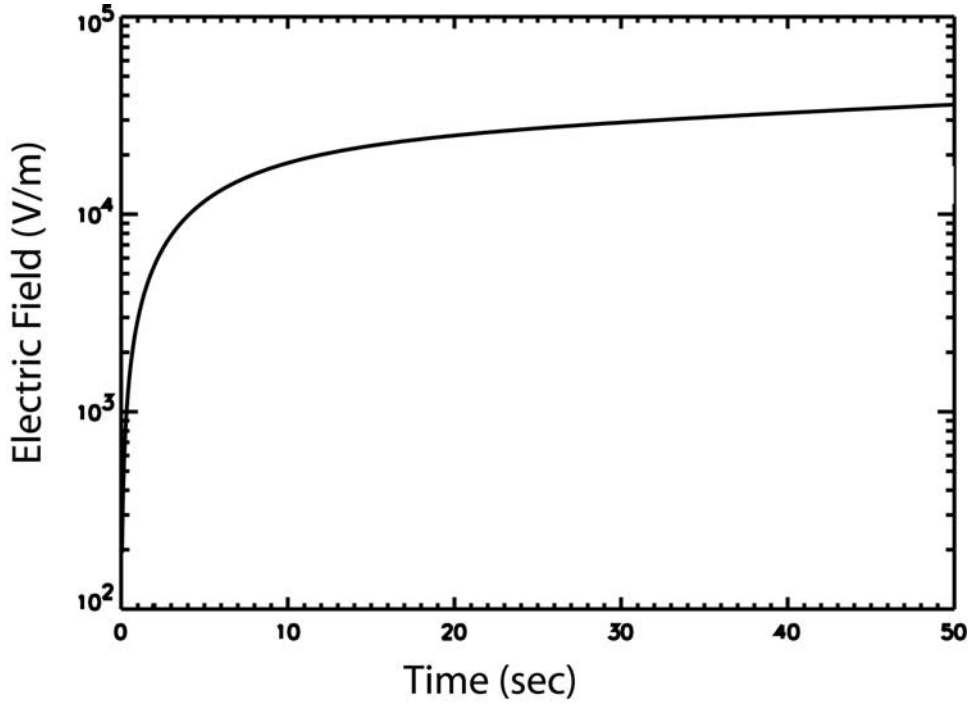

Figure 3. Development of the electric field in a dust devil with small grains of 1 μm radius and 50 particles cm^{-3} and large grains of 20 μm radius and 1 particle cm^{-3} in a 7 m/s wind. The case is run for a Martian-like atmosphere, with near-surface conductivity of 2.5×10^{-12} S m^{-1} and atmospheric density of 1.6×10^{-2} kg m^{-3}.

currents can become comparable to the currents carried by the grains, thereby reducing the *E* field. In essence, these coronal currents act to "short out" the charge centers formed by the separating grains. A second saturating mechanism is the full spatial separation of the small grains from the large grains, effectively reducing the collision frequency, ν, to zero. As a consequence, the $Q_L'\Delta v$ driving term in equation (4) goes to zero as well. Further, the

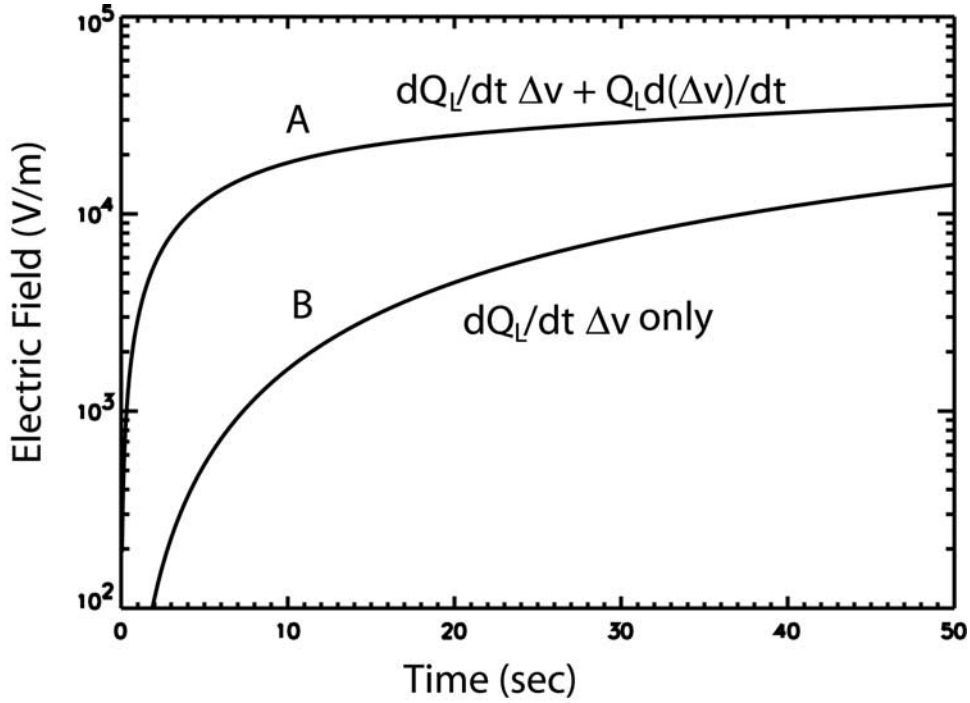

Figure 4. Same case as Figure 3 shown in curve A, while the grain acceleration current that drives the differential equation (4) is removed in curve B. Note that the grain acceleration current dominates the development of E in the early period of formation.

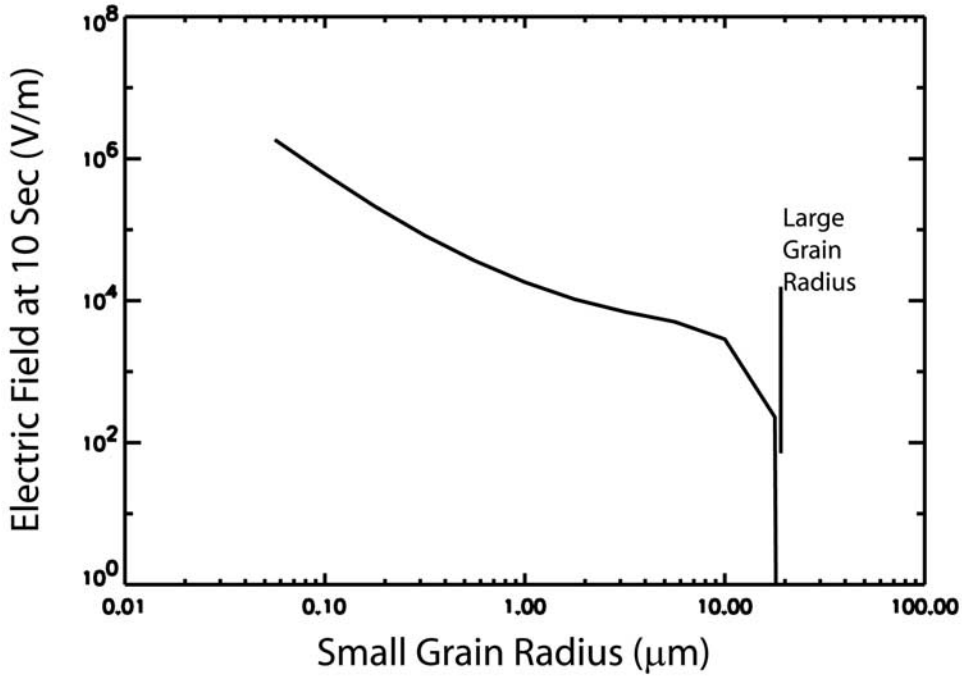

Figure 5. Electric field at 10 s as a function of small grain radius. Note that the electric field drops to zero as the size of the small grains approaches that of the large grains. The atmospheric parameters are the same as that in Figure 3, with only the small-grain radius changing.

second term also tends to zero for long times because $\Delta v'$ approaches zero (Δv is a constant at long times, see Figure 2) making the driving term disappear. Both of these effects could be modeled using time-varying atmospheric currents and collision frequencies, but is beyond the scope of the presentation herein of the more fundamental connection of E and wind velocity.

[27] As stated in the introduction, mass stratification of small and large grains (of opposite polarity) in a dust devil is critical for the development of the electrostatic field. To test the efficiency of mass stratification, we vary the small-grain radius to determine the associated electric field (at t = 10 s). The results are presented in Figure 5. Specifically, the field decreases as grain radius increases, dropping to zero when both small and large grains have 20 μm radii. In essence, as the smaller grains become larger, their lift velocity is steadily decreasing, making Δv and $\Delta v'$ in equation (4) progressively smaller. When both are of the same size, the grains are not effectively separated in space (Δv and $\Delta v'$ are zero), making the dust cloud neutral with an electric field of zero.

[28] Figure 6 shows the variation of the electric field under varying wind speeds. At large values of velocity, the dependency of electric field with prevailing wind speeds is linear, with the rate of charge grain separation and electric field growth increasing with progressively greater wind speeds.

[29] Some caution should be used in applying the results of Figure 6 at low velocities. First, the assumed vertical wind force described in equation (6) holds for relatively fast flows. Second, if vortex vertical wind speeds are low but vortex tangential wind speeds are high, grain lifting could become dominated by horizontal wind shear stresses. *Greeley et al.* [2003] found that for particle sizes >60 μm, the dominant lift mechanism in vortices was shear stresses with particle dynamics mimicking those found in boundary layers. However, smaller particles (<10 μm) were found to obtain lift directly from the associated pressure gradient (with shear stress forces being secondary). Thus, at low velocities shown in Figure 6, other unmodeled effects may occur making the estimates less accurate than at higher velocities. While beyond the current scope, a more advanced multidimensional analysis would include the effect of horizontal shear stresses in the grain lifting process, thereby making the model more applicable to larger sand-sized particles (>60 μm) that are strongly influenced by such shear stresses.

[30] Figure 7 is a most interesting plot of *E* field versus local atmospheric conductivity, σ. The *E* field after 10 s for identical dust devils for Earth-like and Mars-like atmospheric conductivities is identified in Figure 7. Figure 7 indicates that for conductivities below about 10^{-13} S m^{-1}, the atmospheric currents (σE) are small and have little or no impact on the electric field generated from current in small/large-grain separation ($n_L Q_L \Delta v \gg \sigma E$). In contrast, for conductivities above 10^{-12} S m^{-1}, the atmospheric currents become comparable to the currents in grain separation ($\sigma E \sim n_L Q_L \Delta v$), and act to 'short out' the electrostatic field. These "return" currents act to retard the development of the electric field by neutralizing the separating grain charge with nearly equal and opposite amounts withdrawn from the atmospheric reservoir.

[31] From Figure 7 we conclude that on Earth, atmospheric currents have a noticeable effect on dust devil electric field development, but will not destroy the field formed via separating grain currents. On Mars, the atmo-

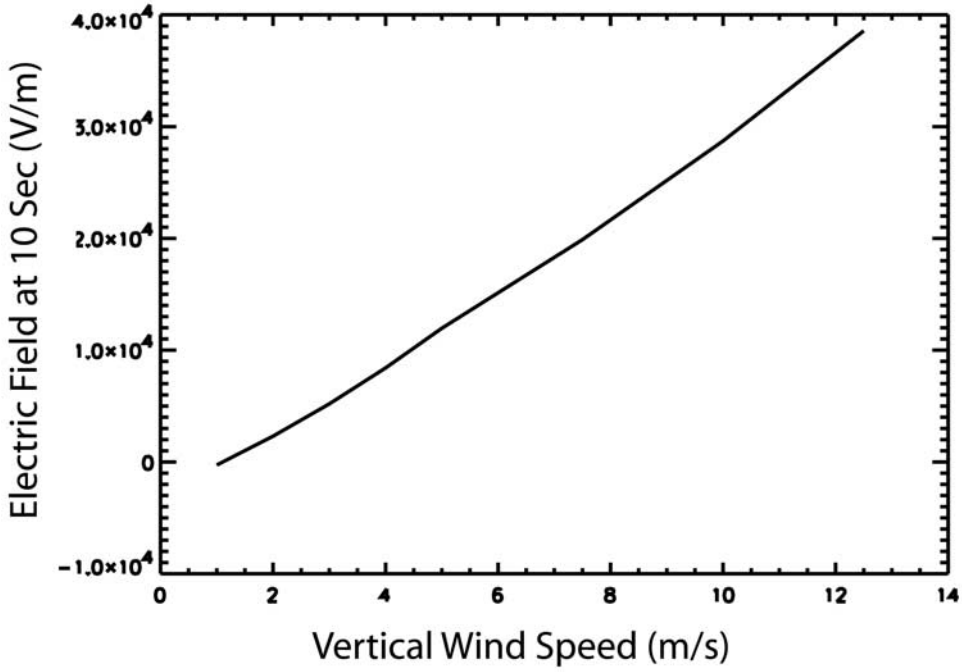

Figure 6. Electric field at 10 s as a function of vertical wind speed. Note that the electric field varies linearly with speed. The atmospheric parameters are the same as that in Figure 3, with only the wind speed changing.

spheric return currents retard the development in a substantial way, to about 1/2 the "no dissipation" case at low conductivities. However, there is still the development of an electrostatic field formed by small/large-grain charge separation (in the case modeled, to 18 kV m^{-1} after 10 s). This result assumes that the Martian atmospheric conductivity is $\sim 2.5 \times 10^{-12}$ S m^{-1} [*Cummer and Farrell*, 1999], a conductivity based on modeling. If the conductivity is substantially larger (e.g., 100 times larger), then the electrostatic field in a Martian dust devil/storm may be

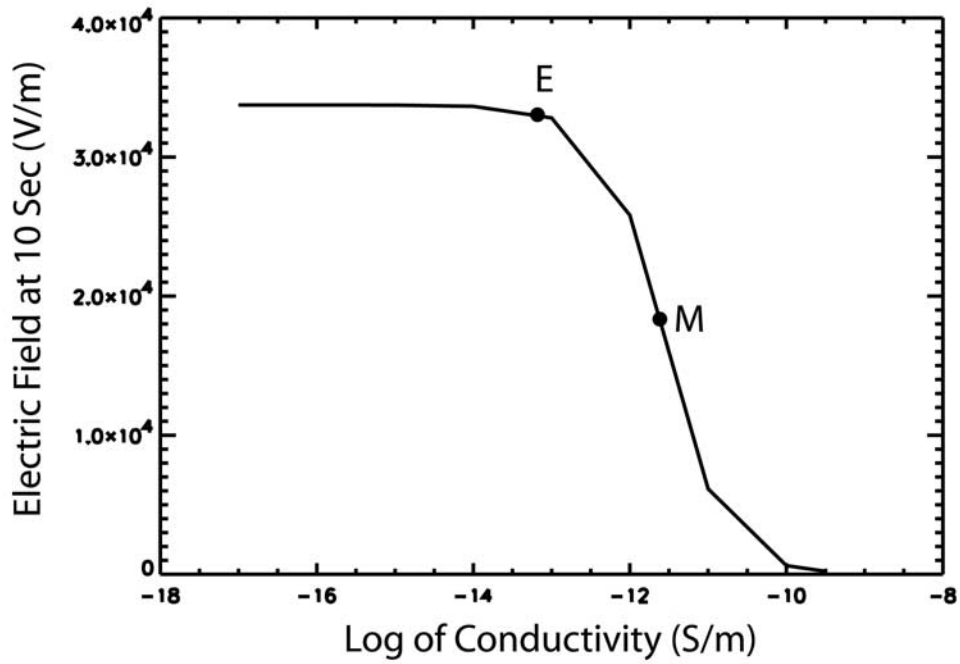

Figure 7. Electric field at 10 s as a function of atmospheric conductivity. Both the Earth-like and Mars-like cases are shown. Note that as atmospheric conductivity gets large, the charge in the atmospheric reservoir is capable of neutralizing the dust devil electrostatic field. The atmospheric parameters are the same as that in Figure 3, with only conductivity changing.

shorted out via atmospheric return currents. In this high-conductivity situation, rather than a large-scale electric field, one might anticipate shorter-lived electric field fluctuations in association with local imbalances between the separating grain charge and atmospheric current influx.

[32] While our model cannot account for breakdown (need to add impulsive atmospheric current source in equation (2)), we can infer its behavior via Figure 7. Specifically, if the electric field increases above breakdown levels, a local corona should develop that raises the local atmospheric conductivity by providing more free electrons. As indicated in Figure 7, as the local atmospheric conductivity increases, the electric field decreases, possibly acting to reduce the electric field back to prebreakdown levels. The coronal current neutralizes the excess dust grain currents, thereby making the system self-regulating.

[33] Equations (7) and (8) ignored the small effect of grain-grain collisions on grain motion. To consider this effect, the formalism of equations (7)–(16) was rederived assuming collisions between large and small grains affected small-grain trajectories. To accommodate this effect, a term in the form of $-(v_S - v_L)/\tau$ was added to the small-grain equation of motion, equation (7), where $1/\tau$ is the large-small-grain collision frequency, ν. It was found that the expressions for P_S, M_S, and R_S (equations (13)–(15)) were essentially unchanged (for the cases run in Figures 2 and 3 there are ~2% decreases), but that W_S (equation (16)) that defines the exponential increase in speed is now $W_S = (4(g - V/\tau)\, c_S)^{1/2}$ (which for the cases in Figures 2 and 3 is a reduction in W_S of 40%). Integrating these changes into the small-grain velocity, v_S, (equation (11)), we find that the velocity of the small grains is basically unchanged when considering long times. However, the linear-like ramp up in speed has a slight reduction in slope (slightly slower ramp-up period). In essence, the analysis is altered only in a minor way when these collisions are included in the fluid dynamics.

5. Conclusions

[34] As described previously by *Farrell et al.* [2003], the electrostatic formalism presented in equations (1)–(4) has some parallels to that used to model the electrostatic field in thunderstorms [*Mathpal et al.*, 1980; *Kuettner et al.*, 1981; *Volland*, 1984]. In the terrestrial induction case, light ice and heavy water and graupel collide within a thunderstorm, with the light ice blown upward with positive charge and heavy water and graupel move downward with negative charge. This charge generation creates an overall electric dipole moment in the thundercloud with electric fields in excess of 100 kV m^{-1}. The thunderstorm electrostatic formalism has been modified herein to incorporate dust grain-grain tribo-electric charging (as opposed to ice/water induction charging in thunderstorms) and to incorporate a time-varying differential velocity, making this electrostatic analysis unique from that applied previously.

[35] We have assumed two grain-sized components in many of our examples: small grains of 1 μm radius and large grains of 20 μm radius. The use of two discrete grain radii demonstrates the growth of the electric field and can certainly be tested in a laboratory (since grain size can be controlled). However, the two species approach is unrealistic in field applications where grain size distributions are representative by a continuum. To move from a size discrete to size continuum formalism, equation (2) needs to be modified to include the current contribution from particles of all sizes (e.g., $\int f(r)\, Q(r)\, v(r)\, dr$, where f(r) is the number density of grains between radius $r - dr/2$ and $r + dr/2$). This inclusion makes the driver of differential equation (4) an integral over the particle radius. One can solve this more complicated system by using a set of discrete currents to represent the integral, assuming an f(r) a priori. Another way of solving this continuum problem is to apply a density-weighted solution from *E* fields at discrete sizes, like that in Figure 5, to the continuum described by f(r). Thus, while we have solved for the "degenerate" two-radii case, the solutions herein allow for an estimate of the *E* field generated from a continuum of sizes.

[36] Equation (3) employs a quasi-neutrality assumption that all charges remained conserved in the system. This assumption is clearly idealized and is used to ease the formalism. In reality, dust devils and dust storms are open systems and there is no reason to believe that charge remains conserved. For example, positive charged grains saltating near the ground may be lost in the dust devil system as it moves over the terrain. This charge loss represents a break in quasi-neutrality and another current that can be added to equation (2), along with any impulsive currents associated with discharges. A more advanced model could incorporate these currents.

[37] By design, we have employed small grains that are not susceptible to shear stress forces, thereby allowing the use of equations (7)–(8) in describing the primary particle dynamics. As described by *Greeley et al.* [1981, 2003], grains greater than 60 μm tend to get lift from this horizontal force and consequently, our formalism breaks down in the description of sand-sized grains. In the future, a more advance model could incorporate these shear stress forces as well.

[38] In summary, our objective was to combine fluid dynamics with electrostatics to derive the electrostatic field expected within a dust devil/storm, in essence demonstrating that the electric fields derive their causality on meteorological factors like vertical winds. The resulting electric field is dependent upon grain properties (density, radius) and vertical wind speed. Given estimates of these variables, a prediction of the electric field within the dust devil can be obtained. Example cases were run for a dust devil on Mars, and the electric field was found to vary linearly with wind speed, decrease sharply as grain radii become comparable, and exponentially decay with atmospheric conductivities above 10^{-13} S m^{-1}. We found that when atmospheric conductivities are very large ($>10^{-11}$ S m^{-1}), the charge residing in the atmosphere can neutralize the electric field established by the separating grains, thereby "shorting out" the electric field in the dust devil. On Mars, we anticipate an electrostatic fields to develop from separating large and small grains, to values approaching local breakdown.

[39] **Acknowledgments.** This work was funded by a NASA/Mars Fundamental Research Program (MFRP) award, which is heartily acknowledged. This work also gratefully acknowledges the early investigators in the field of dust devil/storm electrification, including Freier, Crozier, and especially Eden, Vonnegut, and Mills, who were 30 years ahead of their time.

References

Anderson, R. S. (1987), Eolian sediment transport as a stochastic process: The effects of a fluctuating wind on particle trajectories, *J. Geol.*, *95*, 497.

Cantor, B. A. (2003), Observations of Martian dust storm activity, paper presented at Sixth International Conference on Mars, Calif. Inst. of Technol., Pasadena, Calif.

Crozier, W. D. (1964), The electric field of a New Mexico dust devil, *J. Geophys. Res.*, *69*, 5427.

Cummer, S. A., and W. M. Farrell (1999), Radio atmospheric propagation on Mars and potential remote sensing applications, *J. Geophys. Res.*, *104*, 14,149.

Delory, G. T., W. M. Farrell, B. Hillard, N. O. Renno, P. Smith, J. R. Marshall, and A. Eatchel (2002), The electrical structure of terrestrial dust devils: Implications of multiple vertical measurements of the electric field, *Eos Trans. AGU*, *83*(47), Fall Meet. Suppl., Abstract P51A-0335.

Desch, S. J., and J. N. Cuzzi (2000), The generation of lightning in the solar nebula, *Icarus*, *143*, 87.

Eden, H. F., and B. Vonnegut (1973), Electrical breakdown caused by dust motion in low pressure atmospheres: Consideration for Mars, *Science*, *180*, 962.

Edgett, K. S., and M. C. Malin (2000), Martian dust raising and surface albedo controls: Thin dark (and sometimes bright) streaks and dust devils in MGS high resolution images, *Lunar Planet. Sci.*, *XXXIII*, abstract 1073.

Ette, A., II (1971), The effect of Hermattian dust on atmospheric electric parameters, *J. Atmos. Terr. Phys.*, *33*, 295.

Farrell, W. M., G. T. Delory, S. A. Cummer, and J. R. Marshall (2003), A simple electrodynamic model of a dust devil, *Geophys. Res. Lett.*, *30*(20), 2050, doi:10.1029/2003GL017606.

Farrell, W. M., et al. (2004), Electric and magnetic signatures of dust devils from the 2000–2001 MATADOR desert tests, *J. Geophys. Res.*, *109*, E03004, doi:10.1029/2003JE002088.

Freier, G. D. (1960), The electric field of a large dust devil, *J. Geophys. Res.*, *65*, 3504.

Greeley, R., et al. (1981), Dust storms on Mars: Considerations and simulations, *Geophys. Soc. Am. Spec. Pap.*, *186*.

Greeley, R., et al. (1992), Martian eolian processes, sediments and features, in *Mars*, edited by H. H. Keifer et al., p. 730, Univ. of Ariz. Press, Tucson.

Greeley, R., M. R. Balme, J. D. Iversen, S. Metzger, R. Mickelson, J. Phoreman, and B. White (2000), Martian dust devils: Laboratory simulations of particle threshold, *J. Geophys. Res.*, *108*(E5), 5041, doi:10.1029/2002JE001987.

Houser, J. G., W. M. Farrell, and S. M. Metzger (2003), ULF and ELF magnetic activity from a terrestrial dust devil, *Geophys. Res. Lett.*, *30*(1), 1027, doi:10.1029/2001GL014144.

Kuettner, J. P., et al. (1981), Thunderstorm electrification-inductive or non-inductive?, *J. Atmos. Sci.*, *38*, 2470.

Marshall, J. R. (1994), Particle dispersion experiment (PDE): Preliminary results from the USML-1 glovebox, *NASA CP 3272*, 717.

Mathpal, K. C., et al. (1980), Precipitation-powered mechanisms of cloud electrification, *Rev. Geophys.*, *18*, 361.

Melnik, O., and M. Parrot (1998), Electrostatic discharge in Martian dust storms, *J. Geophys. Res.*, *103*, 29,107.

Mills, A. A. (1977), Dust cloud and frictional generation of glow discharges on Mars, *Nature*, *268*, 614.

Murphy, J. R., and S. Nelli (2002), Mars Pathfinder convective vortices: Frequency of occurrence, *Geophys. Res. Lett.*, *29*(23), 2103, doi:10.1029/2002GL015214.

Renno, N. O., and H. B. Bluestein (2001), A simple theory for waterspouts, *J. Atmos. Sci.*, *58*, 927.

Renno, N. O., and A. P. Ingersoll (1996), Natural convection as a heat engine: A theory for CAPE, *J. Atmos. Sci.*, *53*, 572.

Renno, N. O., M. L. Burkett, and M. P. Larkin (1998), A simple thermodynamical theory for dust devils, *J. Atmos. Sci.*, *55*, 3244.

Renno, N. O., A. A. Nash, J. Lunine, and J. Murphy (2000), Martian and terrestrial dust devils: Test of a scaling theory using Pathfinder data, *J. Geophys. Res.*, *105*, 1859.

Renno, N. O., et al. (2004), MATADOR 2002: A pilot field experiment on convective plumes and dust devils, *J. Geophys. Res.*, *109*, E07001, doi:10.1029/2003JE002219.

Ryan, J. A., and R. D. Lucich (1983), Possible dust devils, vortices on Mars, *J. Geophys. Res.*, *88*, 11,005.

Schmidt, D. A., et al. (1998), Electrostatic forces on saltating sand, *J. Geophys. Res.*, *103*, 8997.

Sickafoose, A. A., J. E. Colwell, M. Horányi, and S. Robertson (2001), Experimental investigations on photoelectric and triboelectric charging of dust, *J. Geophys. Res.*, *106*, 8343.

Smith, P. H., and M. T. Lemmon (1999), Opacity of the Martian atmosphere measured by the imager for Mars Pathfinder, *J. Geophys. Res.*, *104*, 8975.

Thomas, P., and P. J. Gierasch (1985), Dust devils on Mars, *Science*, *230*, 175.

Volland, H. (1984), *Atmospheric Electrodynamics*, Springer, New York.

Zurek, R. W., et al. (1992), Dynamics of the atmosphere of Mars, in *Mars*, edited by H. H. Keifer et al., p. 799, Univ. of Ariz. Press, Tucson.

S. A. Cummer, Department of Electrical and Computer Engineering, Duke University, Hudson Hall, Room 130, Box 90291, Durham, NC 27708, USA.

G. T. Delory, Space Sciences Laboratory, University of California, Berkeley, CA 94720, USA.

W. M. Farrell, NASA Goddard Space Flight Center, Mail Code 695, Greenbelt, MD 20771, USA. (william.farrell@gsfc.nasa.gov)

J. R. Marshall, SETI Institute, 515 N. Whisman Road, Mountain View, CA 94043, USA.

N. Renno, Atmospheric, Oceanic and Space Sciences, University of Michigan, 2455 Hayward St., Ann Arbor, MI 48109-2143, USA.